"RECENT ADVANCES IN ASTRONOMY AND ASTROPHYSICS"
7th International Conference of the Hellenic Astronomical Society, Lixourion, Kefalinia Island, GREECE
(8 - 11 September 2005) (ed. N. SOLOMOS)
AIP CONFERENCE PROCEEDINGS 848 (2006), pp 874 - 882

Detection of slopes of linear and quasi-linear structures in noisy background, using 2D–FFT

P. Tsitsipis[*], A. Kontogeorgos[*], X. Moussas[†], P. Preka–Papadema[†], A. Hillaris[†,**], V. Petoussis[*], C. Caroubalos[†], C. E. Alissandrakis[‡], J.-L. Bougeret[§] and G. Dumas[§]

[*]*Technological Education Institute of Lamia, Lamia, Greece*
[†]*University of Athens, 15783 Athens, Greece*
[**]*Hellenic Naval Academy, Piraeus 18503, GREECE*
[‡]*University of Ioannina, 45110 Ioannina, Greece*
[§]*Observatoire de Paris, CNRS UA 264, 92195 Meudon Cedex, France*

Abstract. We present a fast algorithm for slope detection on grey scale images, based on 2D–FFT, which may be used for line or edge detection. Our approach is based on the calculation of *"energy"* per direction of the image, thus obtaining the Energy Spectrum on Slope (α). This exhibits local maxima at the points where α equals the slopes of linear or quasi–linear segments within the image, yet it is not affected by their position within it. The process thus outlined was motivated by the study of astrophysical images (Solar Dynamic Radio Spectra) which necessitated the introduction of a method for fast extraction of *drifting structures*, since they appear as linear or quasi linear segments on these spectra.

Keywords: Solar activity; Corona; Radio; Radiation and spectra; Solar electromagnetic emission
PACS: 96.60.Q; 96.60.P; 95.85.Bh; 96.25.Tg; 96.60.Tf

INTRODUCTION

The Solar Radiospectrograph (ARTEMIS-IV[1]) is in operation at the Thermopylae Satellite Communication Station since 1996 (cf. [1], [4]). The observations extend from the base of the Solar Corona (650 MHz) to about 2.7 Solar Radii (20 MHz) with time resolution 1/10-1/100 sec. The instruments recordings, being in the form of *"Dynamic Spectra"*, depict the variations in the bursts radiation intensity, represented by pixel brightness, in terms of time and logarithm of frequency which form, respectively, the x and y axis of an image. The frequency is characteristic of a certain layer of the solar atmosphere and proportional to the square of the electron number density at that level; thus the logarithm of the frequency is proportional to the layer's height. This is due to the almost barometric (exponential) scaling of the coronal density near the solar surface. The solar radio bursts are broadly classified according to the form of their dynamic spectrum to *"drift bursts"* and *"continua"*; the former being narrow band structures drifting in frequency with time, the latter broadband forms covering most of the spectral range simultaneously.
The *"continua"* family of bursts often excibits *"fine structure"*, which may become ac-

[1] Appareil de Routine pour le Traitement et l' Enregistrement Magnetique de l' Information Spectral

"RECENT ADVANCES IN ASTRONOMY AND ASTROPHYSICS"
7th International Conference of the Hellenic Astronomical Society, Lixourion, Kefalinia Island, GREECE
(8 - 11 September 2005) (ed. N. SOLOMOS)
AIP CONFERENCE PROCEEDINGS 848 (2006), pp 874 - 882

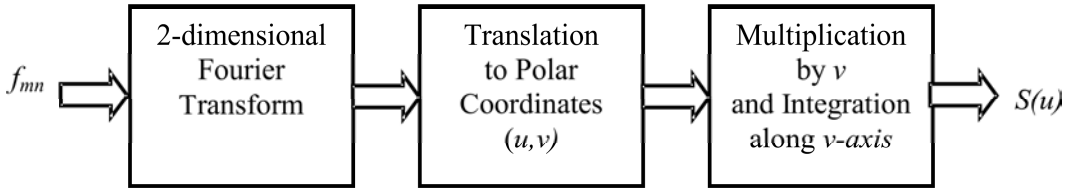

FIGURE 1. Representation of the algorithm for derivation of *angular spectra*.

centuated once the continuum background is suppresed. Certain classes of fine structure features appear in form of groups of drifting elements.
This outlines the importance of the detection of linear segments on dynamic spectra and the necessity of the introduction of the appropriate algorithms, since drifting structures trace the path of an exciter ascending at an almost constant velocity within the solar atmosphere, they form linear segments on the dynamic spectra.
In [5] an efficient method based on Fast Fourier Transform was proposed. The basic idea was the calculation of energy density as a function of angle, with the peaks of *"energy"* per direction on the image indicating, in a statistical sense, the *"dominant"* slopes of linear or quasi linear segments within the image. Certain applications of this algorithm on ARTEMIS–IV dynamic spectra are outlined in this report.

DEFINITION OF THE ANGULAR ENERGY DENSITY–OUTLINE OF THE ALGORITHM

Definition of the Angular Energy Density based on 2D–FFT

An image, or a dynamic spectrum in this case, may be represented by the function $f(x,y)$ of pixel brightness in terms of image coordinates; we may calculate the total *energy* of the image integrating over x and y. Furthermore, using the Parsevals Theorem we can rewrite the resulting integral in Fourier space:

$$\int\int \|f(x,y)\|^2 dxdy = \int_{-\infty}^{\infty}\int_{-\infty}^{\infty} \|F(\xi_1,\xi_2)\|^2 d\xi_1 d\xi_2 = 2\int_0^{\pi} d\theta \int_0^{\infty} \|F(\xi,\theta)\|^2 \xi d\xi \qquad (1)$$
$$\xi_1 = \xi\cos(\theta),\ \xi_2 = \xi\sin(\theta)$$

where, in the last term of equation 1 we have changed from cartesian (ξ_1,ξ_2) into polar (ξ,θ) coordinates in Fourier space. We may define the *"Angular Energy Density"* ($S(\theta)$) as follows:

$$\begin{aligned} S(\theta) &= 2\int_0^{\infty} \|F(\xi,\theta)\|^2 \xi d\xi = \frac{dE}{d\theta} \\ &-\pi/2 \le \theta \le \pi/2 \end{aligned} \qquad (2)$$

The *"Angular Energy Density"* represents the amount of *"Energy"* (E) in the (θ,θ+dθ) range and peaks at θ=ϕ_i+π/2 where ϕ_i is the slope of the i^{th} linear segment(cf. [5]). This characteristic is exploited in the proposed process of *slope detection*.

"RECENT ADVANCES IN ASTRONOMY AND ASTROPHYSICS"
7th International Conference of the Hellenic Astronomical Society, Lixourion, Kefalinia Island, GREECE
(8 - 11 September 2005) (ed. N. SOLOMOS)
AIP CONFERENCE PROCEEDINGS 848 (2006), pp 874 - 882

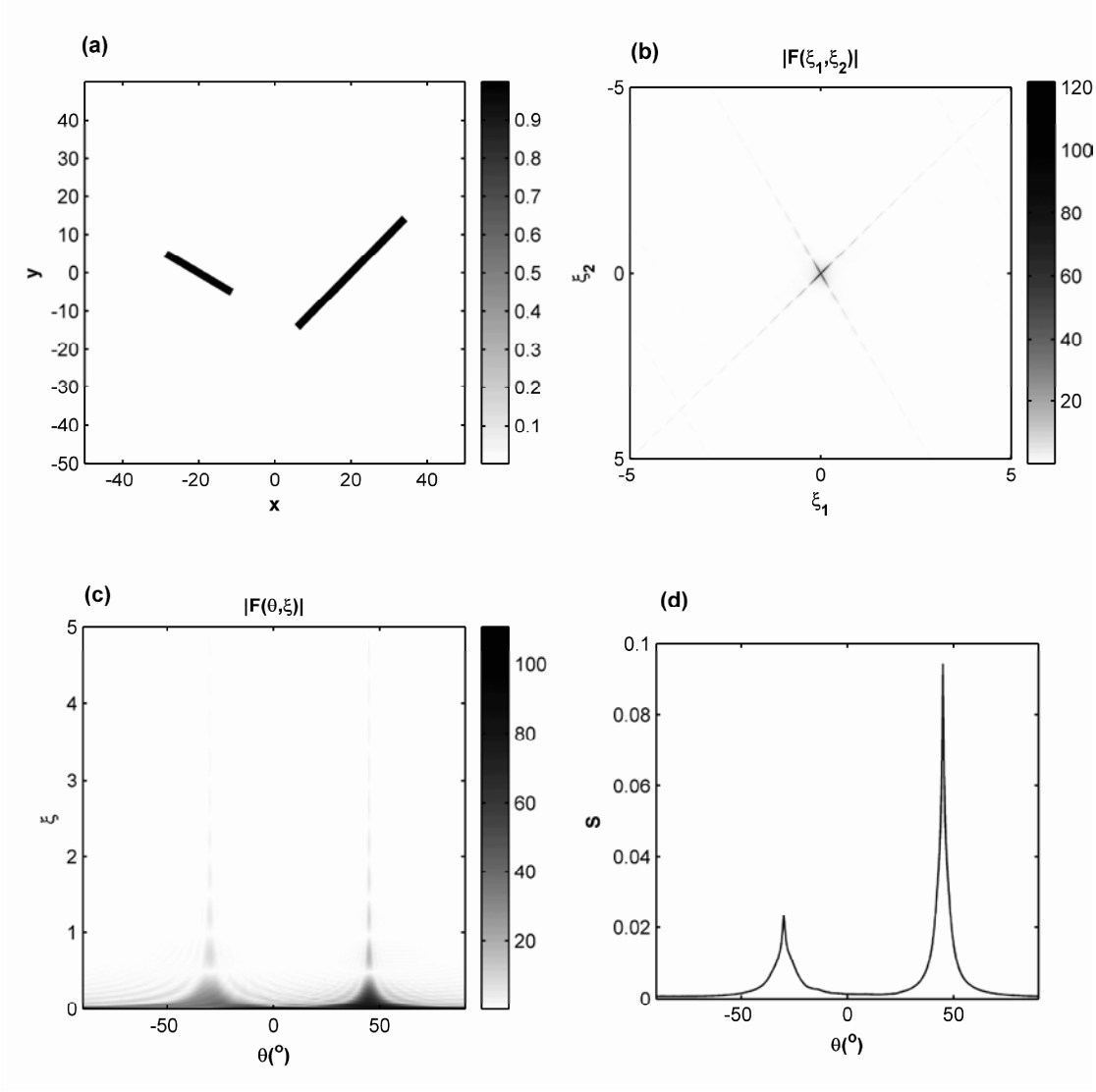

FIGURE 2. (a) Original image representing two line segments in -45^o and 60^o. (b) Two-dimensional Fourier transform of original image (image is rotated by 90^o). Each segment is transformed to a line segment in Fourier space at right angle to the original. (c) The Fourier transform in polar coordinates. (d) The angular spectrum of original image

Discrete Form of the Angular Energy Density

Upon discretization the variables (x,y) may be replased by (m,n), (ξ_1,ξ_2) by (k,l) and (ξ,θ) by (v,u). We have

$$\begin{aligned} F_{k,l} &= \sum_{m=0}^{M-1}\sum_{n=0}^{N-1} f_{m,n}\left(e^{-i\frac{2\pi}{M}}\right)^{mk}\left(e^{-i\frac{2\pi}{N}}\right)^{nl} \\ E_{k,l} &= \tfrac{1}{M\cdot N}\left\|F_{k,l}\right\|^2 \Leftrightarrow \sum_{k=1}^{M}\sum_{l=1}^{N} E_{k,l} = E \end{aligned} \tag{3}$$

"RECENT ADVANCES IN ASTRONOMY AND ASTROPHYSICS"
7th International Conference of the Hellenic Astronomical Society, Lixourion, Kefalinia Island, GREECE
(8 - 11 September 2005) (ed. N. SOLOMOS)
AIP CONFERENCE PROCEEDINGS 848 (2006), pp 874 - 882

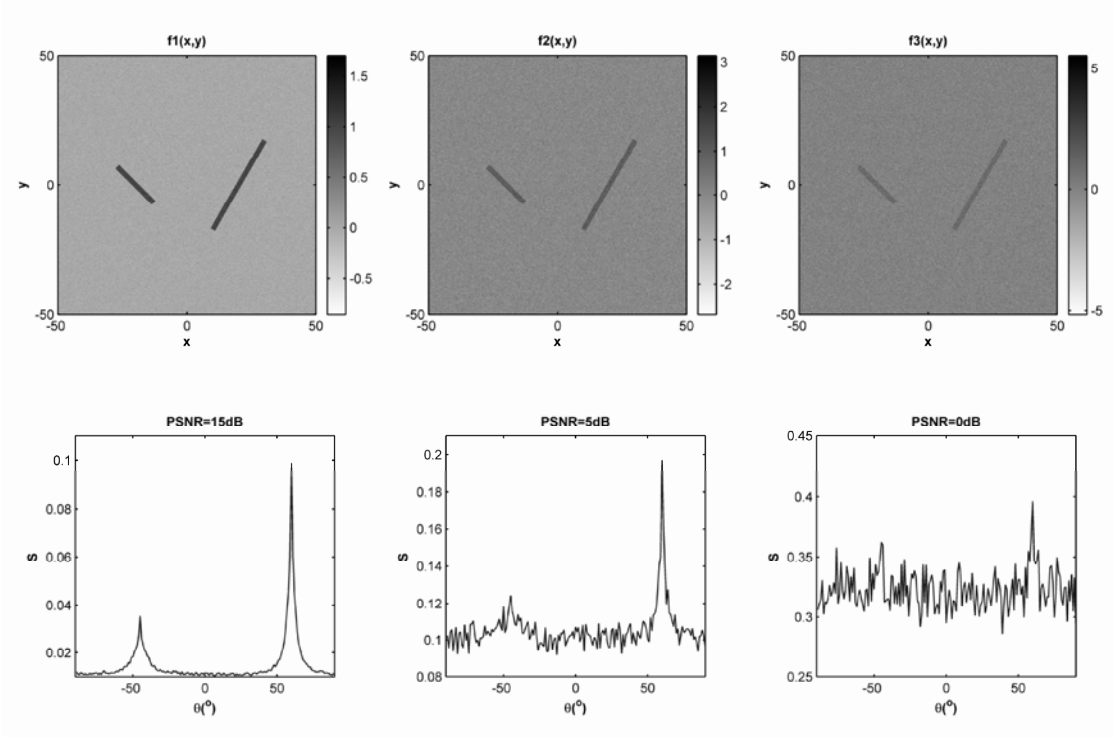

FIGURE 3. Angular spectra of images with noisy backgrounds. Top: Original images with PSNR (Peak Signal to Noise Ratio) of 15, 5 and 0 db respectively. Bottom: The corresponding angular spectra.

where we have assumed that the original function and the corresponding 2D Fourier transform were sampled on a $M \times N$ grid. $F_{k,l}$ stands for the two dimensional discrete Fourier Transform of $f(x,y)$ and $E_{k,l}$ for the *Energy* on pixel (k,l), in Fourier space. In discrete polar coordinates equation 3 assumes the form:

$$E = \sum_{u} S_u = \sum_{u} \frac{2}{\pi N_B^2} \sum_{\upsilon=1}^{N_B} \upsilon \cdot E_{u,\upsilon} \tag{4}$$

where we have taken N_B=$\frac{N}{2} - 1$, under the assumptions $M = N$ and $N_B >> 1$ which do not result in any loss of generality, and S_u stands for the energy along the, discrete, direction u. We note that for the Fourier Transform in polar form the sampling is not uniform as it is the case for the original function and its transform in Cartesian Coordinates, therefore the multiplier υ is used in the summation. Equation 4 constitutes the definition of the *"Angular Energy Density"* in discrete form, which is used henceforward throughout the text. Examples of the computation of the *"Angular Energy Density"* of linear segments on image are presented in Figure 2.

"RECENT ADVANCES IN ASTRONOMY AND ASTROPHYSICS"
7th International Conference of the Hellenic Astronomical Society, Lixourion, Kefalinia Island, GREECE
(8 - 11 September 2005) (ed. N. SOLOMOS)
AIP CONFERENCE PROCEEDINGS 848 (2006), pp 874 - 882

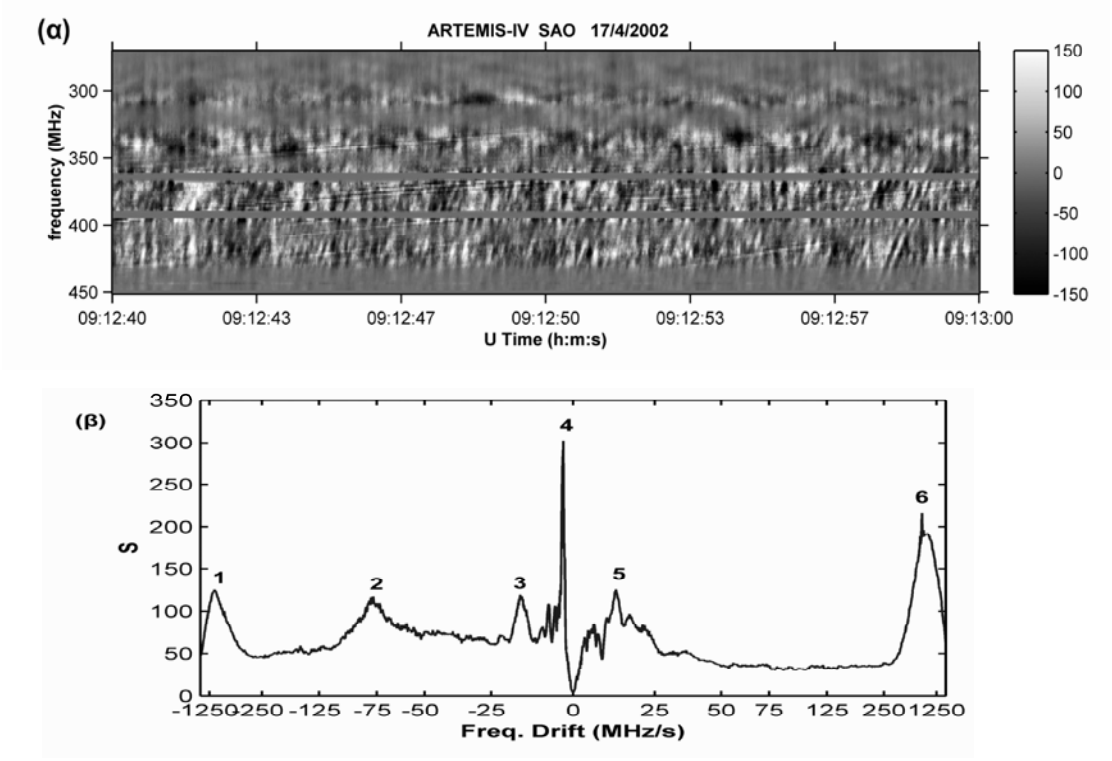

FIGURE 4. Detection of linear segments corresponding to drifting structures on a dynamic spectrum recorded by the ARTEMIS-IV radiospectrograph on the 17 April 2002. Top: Dynamic Spectrum (after an application of high pass filter along the x–axis which has suppressed the background) of a solar continuum; the lines parallel to the time axis represent fixed frequency terrestrial interference; the fine structure consists of pulsations & fibers. Bottom: The application of the *Slope Detection Algorithm*, [5], provides a distribution of pulsation & fiber *Slopes* for the filtered dynamic spectrum; these correspond to the distribution of frequency drift rates for each.

Robustness of the Method in the Presence of Additive White Gaussian Noise

The presence of additive white gaussian noise (AWGN) in the image will increase the mean and variance of backgound level of the *"Angular Energy Density"*. In particular, additive white noise with zero mean and variance equal to σ^2, may raise the *"Mean Square Error"* (henceforward MSE) of a noiseless image with maximum equal to unity to MSE=σ^2.

$$\mathrm{var}[S_u] = \frac{2\sigma^4}{3\pi^2} \cdot \frac{(N_B+1)(2N_B+1)}{N_B^3} \approx \frac{4\sigma^4}{3N_B\pi^2}, N_B \gg 1 \tag{5}$$

This result suggests the use of a reasonable threshold (such as 5σ) in order to discriminate the spectral peaks representing line segments, from the noise spectrum. Hence we have $S_u \geq 10\sigma^2/\pi\sqrt{3N_B}$.

"RECENT ADVANCES IN ASTRONOMY AND ASTROPHYSICS"
7th International Conference of the Hellenic Astronomical Society, Lixourion, Kefalinia Island, GREECE
(8 - 11 September 2005) (ed. N. SOLOMOS)
AIP CONFERENCE PROCEEDINGS 848 (2006), pp 874 - 882

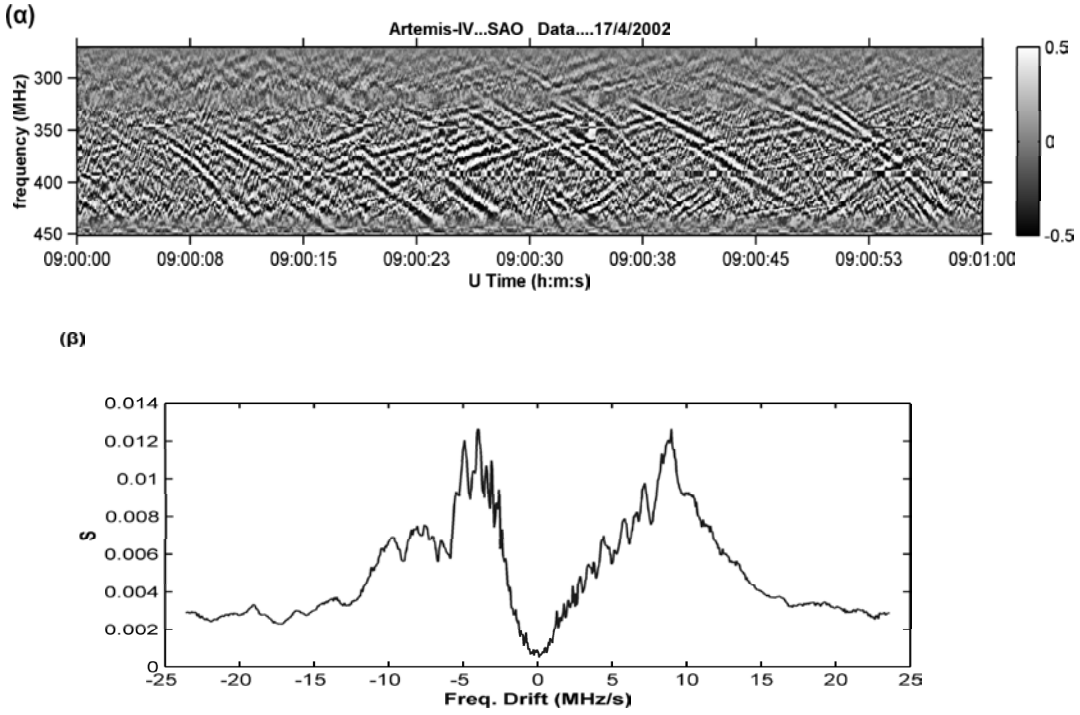

FIGURE 5. Angular energy distribution of fibers on a dynamic spectrum recorded by the ARTEMIS-IV radiospectrograph [2] on the 14 July 2000. Top: Dynamic Spectrum (Continuum background has been suppressed by high pass filtering and terrestrial interference has been eliminated by directional filtering. Bottom: Angular Energy Density of the filtered image.

An example of the angular energy density of two linear segments embedded in a noisy backgound for different signal to noise ratios is excibited in Figure 3.

A more detailed analysis of the edge–detection algorithm, with the appropriate derivation of the above results is presented in [5].

DETECTION OF FINE STRUCTURE APPEARING AS LINEAR SEGMENTS ON SOLAR DYNAMIC SPECTRA

General Description–Application of the Algorithm

Often some part of the image background needs be suppressed in order to enhance the linear structures before their detection, hence an initial stage of high pass filtering is, usually, included. As regards the dynamic spectra of solar radio bursts in particular, the detection of fine structure is customarily obtained by differentiation on time; this however, may introduce loss of information or distortion of the original signal. The use of directional filters to suppress interference at specific angles, such as θ=0 corresponding to fixed frequency terrestrial signals seems promising. Gaussian filters seem also appropriate to this task as they may also suppress slowly varying background

"RECENT ADVANCES IN ASTRONOMY AND ASTROPHYSICS"
7th International Conference of the Hellenic Astronomical Society, Lixourion, Kefalinia Island, GREECE
(8 - 11 September 2005) (ed. N. SOLOMOS)
AIP CONFERENCE PROCEEDINGS 848 (2006), pp 874 - 882

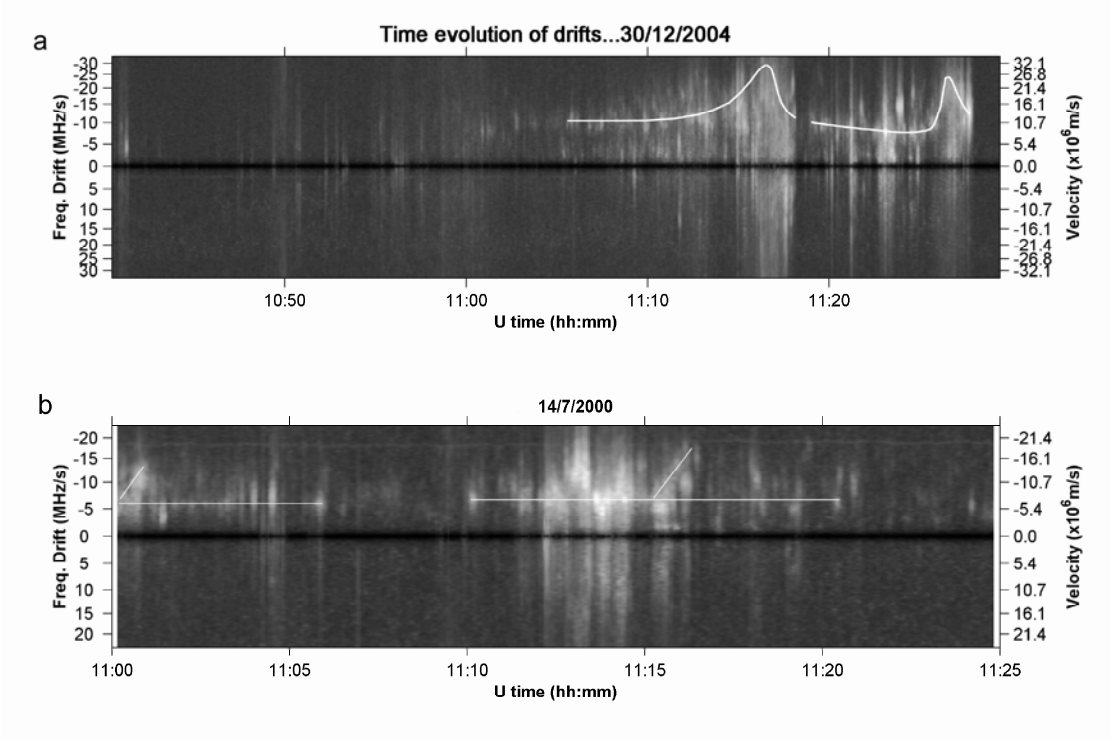

FIGURE 6. Top panel: Evolution of frequency drift rate in a period of 30 minutes during the great solar event of 30–12–2004 in the range 270–450 MHz. The overlayed curve represents the variation of peak frequency drift rate of fibers during this time period. Bottom panel: Same as top panel but for the event of 14–7–2000.

components.

Further more, since the angle θ on a dynamic spectrum does not carry any physical meaning, we can readily replace it by the *slope* (α) of the angular spectrum which is expressed in MHz/sec, if the axis of frequencies[2] is linear or in sec^{-1} if it is logarithmic; the slope represents the radial velocity of the drifting structure exciter as it traverses the solar corona. Suffice it to note that $\alpha \propto \tan(\theta)$, hence the transition is straightforward.

An application of detection and measurement of frequency drifts is represented in Figures 4 and 5; after the removal of the continuous background a composite fine structure arises including intermediate drift bursts (fibers) and pulsations in the former and complex fiber groups in the latter.

[2] The y–axis usually

"RECENT ADVANCES IN ASTRONOMY AND ASTROPHYSICS"
7th International Conference of the Hellenic Astronomical Society, Lixourion, Kefalinia Island, GREECE
(8 - 11 September 2005) (ed. N. SOLOMOS)
AIP CONFERENCE PROCEEDINGS 848 (2006), pp 874 - 882

The identification of each element within a composite spectral structure and the measurement of individual drift rates is quite difficult, due to the complexity of the recorded spectrum. Yet, the proposed method can detect slopes, corresponding to frequency drift rate, in a statistical sense; the peaks of the angular energy function, in particular, mark the dominant drift rates at each period of observation. In the example presented in Figure 4 significant drift rates of -920, -77, -15.5, -2.9, +12.7 and +700 MHz/sec appear in the time interval 09:12:40–09:13:00 UT on 2002 April 17. The same method is used to detect the dominant frequency drift rates of fibers in a rather complicated spectrum with intertwined fiber groups (Figure 5); in this example the dominant drift rates are -5 and 10 MHz/sec.

The slope detection algorithm presented, may be applied on a, relatively, short window of time *sliding* on a much larger period of activity. The result of this *windowed* algorithm is an *evolution of slope spectra* (cf. Figure 6); the y–axis represents frequency drift and the x–axis time, while the pixel brightness represents the corresponding *Angular Energy Density*. This representation facilitates a comprehensive analysis of the evolution of frequency drift rate, which can lead to estimation and representation of exciter velocity. These graphs could be used to study correlation of exciter velocity with other time varying quantities as total radio flux etc.

CONCLUSIONS

In this report we present a fast algorithm for the detection of linear and quasi–linear structures in gray–scale images. This algorithm introduces the *Angular Energy Density*and detects angular distribution of these structures in images; this statistical approach proves to be very useful in case of a great number of line segments. As is based on Fast Fourier Transform methods, the computational efficiency and, in turn, the rate of estimation are high.

The Noise immunity of the method is satisfactory since PSNR[3] along a given direction angle is greater than a reasonably low threshold.

As regards the detection of solar radio burst fine structure the method proposed appears quite sensitive in slope detection. Since there is a direct correspondence between frequency and height in the solar atmosphere (*Corona*) the slopes of bursts on the time-frequency plane can be, almost immediately, indicate the corresponding velocities of their exciters. This suggests this method as a promising tool in the study of solar radio bursts.

---

[3] Peak Signal to Noise Ratio

"RECENT ADVANCES IN ASTRONOMY AND ASTROPHYSICS"
7th International Conference of the Hellenic Astronomical Society, Lixourion, Kefalinia Island, GREECE
(8 - 11 September 2005) (ed. N. SOLOMOS)
AIP CONFERENCE PROCEEDINGS 848 (2006), pp 874 - 882

ACKNOWLEDGMENTS

This work was partly supported by the Greek Ministry of Education with and *Archimedes II* fund. The ARTEMIS–IV group thanks the Hellenic Telecommunication Organization for hosting the ARTEMIS–IV in the the Thermopylae Satellite Communication Station

REFERENCES

1. C. Caroubalos, D. Maroulis, N. Patavalis, J. L. Bougeret, G. Dumas, C. Perche, C. Alissandrakis, A. Hillaris, X. Moussas, P. Preka–Papadema, A. Kontogeorgos, P. Tsitsipis and G. Kanellakis, *Experimental Astronomy* **11**, 23–32, (2001).
2. C. Caroubalos, C. E. Alissandrakis, A. Hillaris, A. Nindos, P. Tsitsipis, X. Moussas, J. L. Bougeret, C. Bouratzis, G. Dumas, G. Kanellakis, A. Kontogeorgos, D. Maroulis, N. Patavalis, C. Perche, J. Polygiannakis and P. Preka–Papadema, *Solar Physics* **204**, 167–179, (2001).
3. C. Caroubalos, A. Hillaris, C. Bouratzis, C. E. Alissandrakis, P. Preka-Papadema, J. Polygiannakis, P. Tsitsipis, A. Kontogeorgos, X. Moussas, J. L. Bougeret, G. Dumas, C. Perche, *A&A* **413** 1125-1133 (2004).
4. C. Caroubalos, C. E. Alissandrakis, A. Hillaris, P. Preka–Papadema, J. Polygiannakis, X. Moussas, P. Tsitsipis, A. Kontogeorgos, V. Petoussis, C. Bouratzis, J. L. Bougeret, G. Dumas and A. Nindos, *These Proceedings* (2006).
5. P. Tsitsipis, A. Kontogeorgos, A. Hillaris, X. Moussas, C. Caroubalos, P. Preka–Papadema, *Pattern Recognition* (submitted) (2005).